

# Estimating the Density of Thin Polymeric Films Using Magnetic Levitation

Samuel E. Root,<sup>†</sup> Rui Gao,<sup>†</sup> Christoffer K. Abrahamsson, Mohamad S. Kodaimati, Shencheng Ge, and George M. Whitesides\*<sup>‡</sup>



Cite This: *ACS Nano* 2021, 15, 15676–15686



Read Online

ACCESS |



Metrics & More



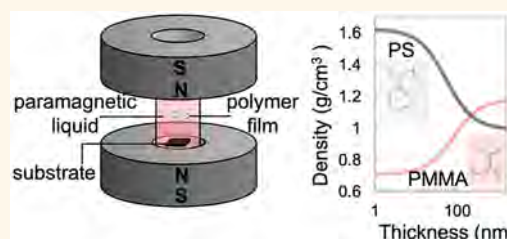
Article Recommendations



Supporting Information

**ABSTRACT:** While the density is a central property of a polymer film, it can be difficult to measure in films with a thickness of  $\sim 100$  nm or less, where the structure of the interfaces and the confinement of the polymer chains may perturb the packing and dynamics of the polymers relative to the bulk. This Article demonstrates the use of magneto-Archimedes levitation (MagLev) to estimate the density of thin films of hydrophobic polymers ranging from  $\sim 10$  to 1000 nm in thickness by employing a substrate with a water-soluble sacrificial release layer to delaminate the films. We validate the performance of MagLev for this application in the  $\sim 1 \mu\text{m}$  thickness range by comparing measurements of the densities of several different films of amorphous hydrophobic polymers with their bulk values of density. We apply the technique to films  $< 100$  nm and observe that, in several polymers, there are substantial changes in the levitation height, corresponding to both increases and decreases in the apparent density of the film. These apparent changes in density are verified with a buoyancy control experiment in the absence of paramagnetic ions and magnetic fields. We measure the dependence of density upon thickness for two model polymeric films: poly(styrene) (PS) and poly(methyl methacrylate) (PMMA). We observe that, as the films are made thinner, PS increases in density while PMMA decreases in density and that both exhibit a sigmoidal dependence of density with thickness. Such changes in density with thickness of PS have been previously observed with reflectometric measurements (*e.g.*, ellipsometry, X-ray reflectivity). The interpretation of these measurements, however, has been the subject of an ongoing debate. MagLev is also compatible with nontransparent, rough, heterogeneous polymeric films, which are extremely difficult to measure by alternative means. This technique could be useful to investigate the properties of thin films for coatings, electronic devices, and membrane-based separations and other uses of polymer films.

**KEYWORDS:** polymer films, magnetic levitation, thin films, interfacial confinement, density



## INTRODUCTION

The density ( $\text{g}/\text{cm}^3$ ) of a polymer film provides a connection between the molecular structure and the macroscopic physical properties (*e.g.*, elastic modulus, glass transition temperature ( $T_g$ ), refractive index, and permeability to gases).<sup>1</sup> The measurement of density in thin ( $< 1000$  nm) polymeric films is difficult to achieve and is thus only reported in the literature for relatively few model systems.<sup>2–7</sup> Moreover, changes in the density of thin polymeric films (especially in films having a thickness on the order of or less than 100 nm) relative to bulk polymers are important in elucidating the role of interfaces and confinement, on the packing and dynamics of the polymer chains, and the overall behavior of the resulting films—including optical, electronic, thermal, and mechanical properties of importance for various applications.<sup>8</sup> Existing techniques for measuring the density of ultrathin films ( $< 100$  nm), such as ellipsometry,<sup>3,5,6</sup> X-ray reflectivity,<sup>3</sup> and quartz crystal microbalance dissolution experiments,<sup>7</sup> are indirect,

model-dependent, or require sophisticated equipment and analyses.

Here, we demonstrated that magneto-Archimedes levitation (MagLev)<sup>9,10</sup> can be used to estimate the average density of thin films ( $\sim 10$ – $1000$  nm) of hydrophobic polymers simply and accurately (Figure 1). We assessed the performance of MagLev by comparing values of densities measured by MagLev to those measured by others using other approaches, including ellipsometry and X-ray reflectivity, and quartz crystal microbalance dissolution experiments.<sup>2–7</sup> MagLev is conceptually and operationally simple, broadly compatible with different

**Received:** June 4, 2021

**Accepted:** August 11, 2021

**Published:** August 17, 2021



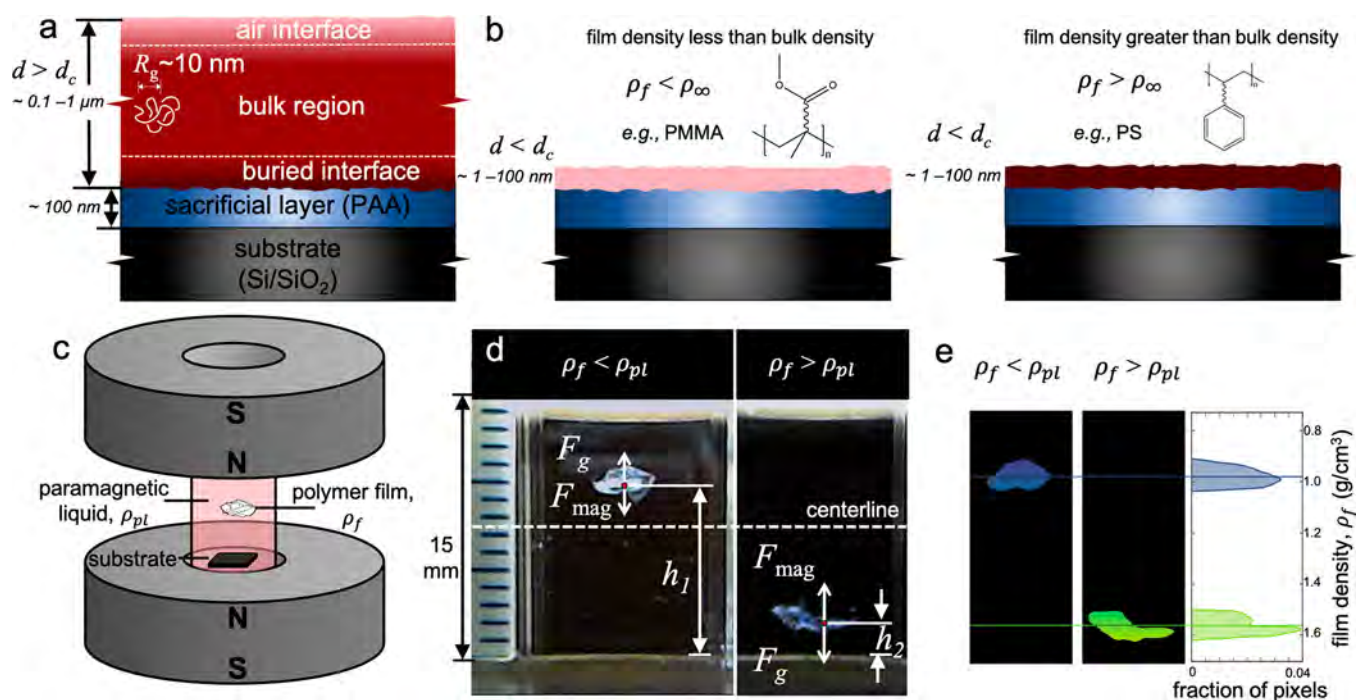


**Figure 1.** MagLev measurement of thin films of polymers. Schematic diagrams of hydrophobic polymer films supported by a substrate containing a water-soluble sacrificial release layer showing (a) a film thicker than the critical thickness,  $d_c$  ( $\sim 100$  nm) and (b) a film thinner than  $d_c$  for the case where the film density decreases relative to the bulk value,  $\rho_f < \rho_\infty$  (PMMA) and for the case where the film density increases relative to the bulk value,  $\rho_f > \rho_\infty$  (PS). The relative thicknesses of the substrate and the sacrificial layer are not drawn to scale, the jagged edges represent thicknesses that are not drawn to scale. (c) A schematic diagram of the axial MagLev device used to levitate thin films and measure their densities. (d) Photographs of two PS films of different thickness and density levitating within the MagLev device. One with a thickness  $> 100$  nm and a density less than the paramagnetic liquid (left,  $\rho_f < \rho_{pl}$ ), levitating to a height,  $h_1$  (mm); and another with a thickness  $\sim 10$  nm and a density greater than the paramagnetic liquid (right,  $\rho_f > \rho_{pl}$ ), levitating to a height,  $h_2$  (mm). In the free body diagrams,  $F_g$  is the buoyancy-corrected gravitational force,  $F_g \equiv (\rho_f - \rho_{pl})gV$ , where  $g$  is the acceleration due to gravity and  $V$  is the volume of the film; and  $F_{mag}$  is the magnetic force. (e) Representations of the photographs after applying an image processing algorithm to estimate the density of the film.

types of polymers, and particularly appropriate for measuring the density of films that are optically opaque, have rough surfaces, or have heterogeneous/composite structures; such characteristics can make density measurements using reflectometry difficult or impossible. The direct measurements of density reported in this work contribute to the body of evidence surrounding the long-standing problem of how interfacial confinement of polymers affects the thermophysical behavior of thin films of them.<sup>11–13</sup> MagLev will be useful for polymer chemists and materials scientists aiming to study and optimize the properties of polymer films for applications including electronic devices, protective coatings, and separations.<sup>14</sup> The details of MagLev are summarized elsewhere,<sup>9,10</sup> including a detailed description of protocols.<sup>15</sup>

**Interfacial Confinement in Polymer Thin Films.** When polymers are confined to films with a thickness,  $d$ , approaching or less than  $\sim 100$  nm, interfacial effects begin to play an important role in determining the physical properties of the polymer film.<sup>8,16</sup> Instead of adopting a three-dimensional random coil conformation (as is typical in the bulk), the polymer chains adopt a conformational structure resembling a two-dimensional random coil.<sup>8,17–19</sup> This reduction in dimensionality couples with interfacial effects due to intermolecular forces to change the ways in which the polymer chains pack and entangle, producing changes in the physical properties of the film.<sup>20</sup> The effects of interfacial confinement on the properties of polymer films were initially observed by

Keddie *et al.*, from measurements of the glass transition temperature ( $T_g$ ) in poly(styrene) (PS) films on Si–H substrates, using temperature-dependent ellipsometry.<sup>11</sup> These initial observations inspired a community of researchers, over the past three decades, to investigate the influence interfacial confinement on the properties of thin polymeric films—with a primary focus on the glass transition.<sup>12,19,21–27</sup>

**Changes in the Glass Transition.** In most cases, the confinement of a polymer to films tens of nanometers thick produces a depression in the glass transition temperature,  $T_g$ , either in a film supported by a substrate<sup>11,23</sup> or in a free-standing film.<sup>22,28</sup> If an attractive polymer–substrate interaction exists, however, an increase in the  $T_g$  can also be observed.<sup>29</sup> These changes in  $T_g$  have also been shown to depend upon the manner in which they are probed, and whether it is a quasi-thermodynamic (*e.g.*, ellipsometry) or kinetic (*e.g.*, inelastic neutron scattering) approach.<sup>16,30</sup> The prevailing theory considers a heterogeneous, stratified film in which the polymer chains in the vicinity of the substrate or the free surface exhibit distinct dynamics, relative to the bulk central region of the film (Figure 1a,b).<sup>31</sup> While the thermophysical behavior at the buried interface is dependent upon the polymer–substrate interaction, at the free surface there is an enhanced segmental mobility and a weaker temperature-dependence of relaxation times at or below the  $T_g$  relative to the bulk.<sup>13</sup>

**Changes in the Mass Density.** Among the thermophysical properties affected by interfacial confinement of thin films is the density ( $\text{g}/\text{cm}^3$ ). Understanding how the density in thin films of polymers is influenced by interfacial confinement is important in elucidating the mechanism underlying the changes in other material properties, such as the glass transition temperature.<sup>3,16</sup> Previous reflectometric measurements of the changes in the density of films of PS with decreasing thickness have produced conflicting results. Initial X-ray reflectivity experiments by Reiter showed a measurable reduction in the density of PS films with a thickness less than the end-to-end distance of the polymers, but the magnitude of the change was not reported, and Reiter noted that X-ray reflectivity is not a very accurate way to determine density of such thin films.<sup>32</sup> Subsequent work by Wallace *et al.* reported no dependence of the density upon on thickness, as measured by twin-neutron reflectivity.<sup>33</sup> Gibaud *et al.* and Ata *et al.* both reported a large increase in density (up to  $\sim 25\%$ ), measured by a combination of X-ray reflectivity and ellipsometry.<sup>2,3</sup> Work by Roth and co-workers has brought into question some of the assumptions underlying the inference of the density from ellipsometry measurements, based on the supposition that these large increases in density are physically unrealistic.<sup>5,6</sup> Specifically, they argue that these unrealistically large values of film density relative to the bulk arise from difficulties in measuring the refractive index of very thin films, and the breakdown in the validity of the assumptions underlying the continuum-scale Lorentz–Lorenz formula (eq 1).<sup>5</sup>

$$\frac{n^2 - 1}{n^2 + 2} = \frac{\alpha N_A}{3\epsilon_0 M_0} \rho \quad (1)$$

which is used to calculate mass density,  $\rho$ , from the measured refractive index,  $n$ , using a known (or assumed) molecular polarizability,  $\alpha$ .<sup>5</sup> In eq 1,  $N_A$  is Avogadro's number,  $M_0$  is the molecular weight of the repeating residue of the polymer, and  $\epsilon_0$  is the permittivity of free space.

Finally, to address such issues related to the inference of density from measurements of refractive index, Giermanska *et al.* have recently introduced a more direct method to measure the density using quartz crystal microbalance dissolution experiments.<sup>7</sup> These experiments provided additional evidence that thin films of PS are denser than the bulk material.

**Changes in the Mechanical Properties.** Simple metrologies, which do not require sophisticated instrumentation or material-specific models, have facilitated the scientific investigation and engineering of polymeric thin films. For example, mechanical metrologies for measuring the tensile modulus, fracture strain, or fracture strength of thin films supported by elastomeric substrates,<sup>34–37</sup> or floating on the surface of water,<sup>38–41</sup> have been particularly useful in the characterization and optimization of flexible and stretchable organic electronic films.<sup>42,43</sup> Such methods have also been used to demonstrate that confined films of PS exhibit a decrease in tensile modulus with thickness, either supported by an elastomeric substrate<sup>44</sup> or floating on the surface of water.<sup>40</sup> A correspondingly simple metrology for the measurement of the density of polymer films that would facilitate the routine measurement of this important property could help elucidate the mechanisms for variations in the  $T_g$  tensile modulus, and other important thermophysical properties.

**Measuring Density with MagLev.** Our group has been developing MagLev as an analytical tool to measure the density of a wide variety of materials, ranging from nonbiological materials such as metals, plastics, and composite materials to biological cells and small organisms.<sup>9,15,45</sup> One class of materials to which MagLev has not yet been applied is films with a thickness of less than  $1 \mu\text{m}$ .

## RESULTS AND DISCUSSION

**Sacrificial Film.** MagLev experiments require the polymeric films to be suspended in a paramagnetic medium; the films should thus be conveniently released from a supporting substrate following their preparation. For some polymers including PS, they can be released easily from a solid substrate, such as a hydrophilic Si/SiO<sub>2</sub> surface.<sup>38</sup> We found that this behavior, however, does not apply broadly to other types of polymers, such as poly(methyl methacrylate) (PMMA). Therefore, we chose to use a water-soluble, sacrificial layer to release the hydrophobic polymeric film. We note that Stone and co-workers recently reported a capillary peeling process that may be of use for experiments such as these that require delamination of a hydrophobic polymer film without a sacrificial-release layer.<sup>46</sup>

We have previously examined the performance of a wide range of polymers suited to serve as a sacrificial layer, and found that poly(acrylic acid) (PAA) ( $\rho_\infty = 1.15 \text{ g}/\text{cm}^3$ ) film offered the best performance in the context of surface micromachining.<sup>47</sup> Other sacrificial layers such as dextrose or poly(methacrylamide) also work well.<sup>47</sup> We tested the influence of the use of PAA on the density of PS measured by MagLev, since PS can be easily delaminated from an Si/SiO<sub>2</sub> surface and does not require a PAA layer. We found that measurements of the density of PS films with and without the use of PAA as a sacrificial layer yielded indistinguishable results for the same processing conditions and thickness of films (measured by stylus profilometry; see *Experimental Methods*). When we characterized the PS films that had been delaminated from PAA using attenuated total reflection infrared spectroscopy, we found no evidence of remaining PAA adsorbed to the PS film (Figure S7). Thus, we assumed, in this study, that the use of a sacrificial layer of PAA would not disturb (at the least not significantly) the behavior of the hydrophobic polymeric films supported on it, in comparison to Si/SiO<sub>2</sub>.

**MagLev System.** We used the “axial” MagLev device<sup>9,48</sup> (Figure 1c, photograph in Figure S10) to carry out the measurements in this study primarily because of its operational simplicity: the hole in the top magnet of the axial MagLev allows for manipulation of the sample from above during levitation, and thus makes it easier to add thin polymer films to the device for density measurement. It offers a  $360^\circ$  view of the sample, and views from the top and bottom of the device. Importantly, the ability to illuminate the levitating film from a source of light above allowed us to obtain higher quality photographs, where the levitating film is clearly visible (Figure 1d). MagLev devices of other configurations, such as the standard configuration,<sup>45</sup> can also be used. Many of the measurements reported here were reproduced by an independent experimenter using the standard MagLev configuration. We used aqueous solutions of MnCl<sub>2</sub> (2.3 or 3.5 M) as the paramagnetic media because they are inexpensive, easily accessible, chemically compatible with hydrophobic polymers, and highly transparent in the visible range (and thus facilitate the viewing of thin polymer films).<sup>48</sup>

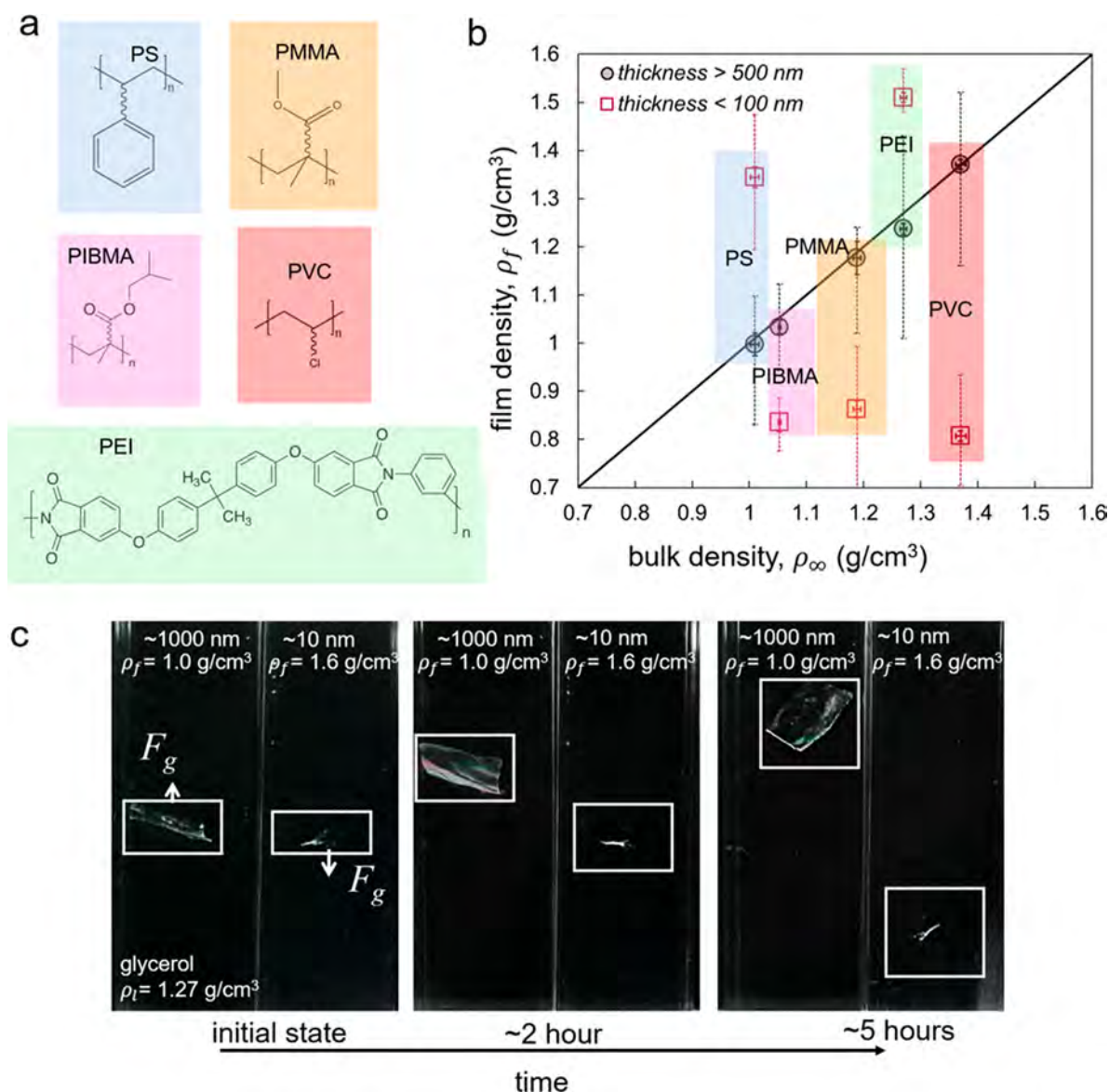


**Figure 2.** Validation of technique and survey of changes in density, which we ascribe to interfacial confinement. (a) Molecular structures of the polymers used to validate the technique. (b) Plot of film density versus bulk density (both measured by MagLev) for four polymers with differences of density between 1–1.4 g/cm<sup>3</sup>. Open black circles represent films with a thickness much greater than 500 nm. Open red squares represent films with a thickness less than 100 nm. Error bars with thick solid lines represent 95% confidence intervals of the mean value of the density determined from the centerline of the levitation height from  $N = 7$  MagLev experiments. Error bars with thin dashed lines represent the density range spanned by an individual film (based on the highest and lowest point from photographs). The bulk densities measured by MagLev agreed with values reported in the literature and by the suppliers of the polymers. (c) Time series of photographs of two polystyrene films of different thickness suspended in a neat glycerol solution ( $\rho_l = 1.27$  g/cm<sup>3</sup>) with no magnetic field, showing that the film of ~1000 nm thickness floats to the top while the film of ~10 nm thickness sinks the bottom.

**Choice of Polymers.** In this study, we chose PS and PMMA as model polymers to examine and measure, by MagLev, the dependence of mass density of films of these polymers upon their thickness. These two polymers are well characterized in the context of interfacial confinement effects, and they show qualitatively opposite behavior: PS increases in density as the thickness decreases, while PMMA decreases in density as the thickness decrease.<sup>3,4,7,32,49,50</sup> Several existing reports of the dependence of density on thickness are in conflict, however, and an alternative method of measurement is required confirm this effect.<sup>3,4,7,32,49,50</sup> We have also used several common polymers that spanned a broad range of bulk densities,  $\rho_\infty$  (1.0–1.4 g/cm<sup>3</sup>), to validate the performance of

the technique: PS ( $\rho_\infty = 1.04$  g/cm<sup>3</sup>), PMMA ( $\rho_\infty = 1.18$  g/cm<sup>3</sup>), poly(vinyl chloride) (PVC,  $\rho_\infty = 1.37$  g/cm<sup>3</sup>), poly(ether imide) (PEI,  $\rho_\infty = 1.27$  g/cm<sup>3</sup>), and poly(isobutyl methyl methacrylate) (PIBMA,  $\rho_\infty = 1.05$  g/cm<sup>3</sup>), see Figure 2.

**Procedure.** Polymer films were spin-cast from either toluene or *N*-methyl-2-pyrrolidone solutions (see Table 1) onto ultraflat silicon substrates containing a native oxide layer (roughness < 0.5 nm as reported by the manufacturer and confirmed by us using atomic force microscopy,<sup>51</sup> Figure S6) and a sacrificial PAA layer (see Experimental Methods for details). The thicknesses of the resulting films were controlled by varying the concentration of the polymer in the solution

**Table 1. Summary of Polymers Employed in This Study**

polymer	acronym	solvent <sup>a</sup>	$M_N$ (kg/mol)	PDI <sup>b</sup>
poly(styrene), polydisperse	PS	toluene	170	2.05
poly(styrene), monodisperse	PS	toluene	111	1.03
poly(methyl methacrylate)	PMMA	toluene	75	2.8
poly(vinyl chloride)	PVC	<i>N</i> -methyl-2- pyrrolidine	>100	>1
poly(ether imide)	PEI	<i>N</i> -methyl-2- pyrrolidine	<i>unknown</i>	>1
poly(isobutyl methyl methacrylate)	PIBMA	toluene	30	>1

<sup>a</sup>Indicates the solvent from which the polymer film was spin-coated.

<sup>b</sup>Polydispersity index (dimensionless), defined as  $M_w/M_n$  (i.e., the ratio of the number-averaged molecular weight to the weight-averaged molecular weight) and represents the distribution of molecular weight in a polymer sample.

and maintaining consistent spin-coating parameters (3000 rpm, 2 min), except for a specific control experiment with PS, in which the spin-coating speed was varied to see if processing history affected the resulting density (it did not). Each sample was subsequently annealed in a vacuum oven well above the glass transition temperature at 160 °C for 12 h (with the exception of the PVC films, which were annealed at 60 °C, due to thermal degradation occurring above this temperature) to remove residual solvent and allow the film to relax any nonequilibrium structures formed during the spin-coating process, following standard protocols from the polymer confinement literature to ensure reproducibility of results.<sup>3,4,22</sup> After cutting the 2" diameter wafers supporting the annealed polymer films into  $\sim 0.25$  cm<sup>2</sup> squares, the sample (Figure 1b) was placed in a cuvette with paramagnetic media in the MagLev device, the sacrificial layer dissolved, and the film settled to a stable levitation height (Figure 1c,d), which could be related to the mass density through the use of a calibration curve (Figures S1,S2). The silicon chip from which the sample delaminated remained at the bottom of the cuvette.

In this work we tested several different procedures of sectioning and releasing the film and found the measured density to be insensitive to the specifics of the experimental protocol (see Experimental Methods for a detailed discussion). The levitation height of the film could be determined by eye or through digital image analysis of the photographs using a ruler in the images for reference (Figure 1e). We observed that the suspended films would often crumple, and we took the levitation height to be the center point of the crumpled film, as estimated by eye (which also matched well with the results of digital image analysis). We found that the center point of the film was consistent from sample to sample, even though the range of density spanned by the crumpled film was typically  $\pm 10\%$  of the mean density (see dashed error bars in Figure 2). We believe the crumpling to be the result of a balance between the buoyant, magnetic forces, and residual internal stresses in the film. The fact that the densities inferred from measurements of  $\sim 1$   $\mu$ m films match well with bulk values suggests that the calibration of the technique with rigid objects and liquid drops is valid for flexible objects and is independent of geometry. The values of density reported in the following sections were taken as the average value of the center point from at least seven different samples. Thicknesses of the films

were measured using stylus profilometry (see Experimental Methods and the Supporting Information for more details). Atomic force microscopy (Figure S7) revealed that the films exhibited a root-mean-squared surface roughness of <1 nm over an area of 25  $\mu$ m<sup>2</sup> before they were delaminated from the silicon substrate.

**Thin Films of Polymers Have Densities That Deviate from Their Bulk Values.** We validated our method by spin-coating films thicker than 500 nm, from concentrated solutions, 100 mg/mL (except for PVC, which exhibited gel-like behavior at this concentration, and was thus spun-cast from solutions containing 50 mg/mL of polymer) and measured the densities of these thick films and the bulk pellets. Figure 2b shows the expected one-to-one correlation between the densities of films and bulk pellets. Next, we spin-cast films of thickness of less than 100 nm from dilute solutions (10 mg/mL) to survey the variations in density caused by interfacial confinement of polymer films (Figure 2b). Interestingly, we observed that, for PS and PEI, the apparent density (as measured by MagLev) increased, while for PMMA, PIBMA, and PVC the apparent density decreased. Photographs of suspended films of PS, PVC, and PEI are included in Figures S3–S5. Tabulated data for all the films tested can be found in Tables S1–S3.

The magnitude of the observed changes in the magnetic levitation height density with film thickness are surprising. There are two possible mechanisms by which these changes could occur: (i) they could result from a change in the mass density of the film, or (ii) they could be the result of some change in the physics of MagLev for thin hydrophobic films levitating within an aqueous paramagnetic medium. The fact that we observed both apparent increases and decreases in density implies that the change is influenced by the chemical nature of the film and not solely the thickness. To clarify the mechanism by which the changes in levitation heights occurred, we performed a float-sink control experiment (Figure 2c): two films of PS were prepared with thicknesses of  $\sim 10$  and  $\sim 1000$  nm. These films were delaminated from the PAA substrate in deionized water and then carefully transferred to cuvettes containing glycerol ( $\rho_1 = 1.27$  g/cm<sup>3</sup>),<sup>52</sup> taking care that there were no bubbles attached to the films (by mechanically agitating the suspended film with a pipet tip until all the visible bubbles detached and floated to the top). After suspending these films at similar heights, they settled under the sole influence of gravity over the course of several hours. As shown in the photographs of Figure 2c, we observed that the  $\sim 1000$  nm film of PS floated toward the surface, while the  $\sim 10$  nm film of PS sank to the bottom, indicating that their densities were less than and greater than the density of glycerol, 1.27 g/cm<sup>3</sup>.<sup>52</sup> This simple experiment suggested that the change in the levitation height with film thickness was the result of a change in the film density and not due to some change in the physics of MagLev for thin films (e.g., a change in magnetic susceptibility due to absorption of the paramagnetic ions into the thin film).

#### Thickness-Dependence of Density of Polymer Films.

To investigate the dependence of the density of films of PS and PMMA on their thickness, we fabricated films of decreasing thickness by spin-coating a set of serially diluted polymer-toluene solutions with concentrations ranging from 1–100 mg/mL. Toluene was chosen because it is a typical solvent that dissolves both PS and PMMA, and it has been used in previous studies.<sup>3,4</sup> Figure 3a,b shows photographs of the levitating

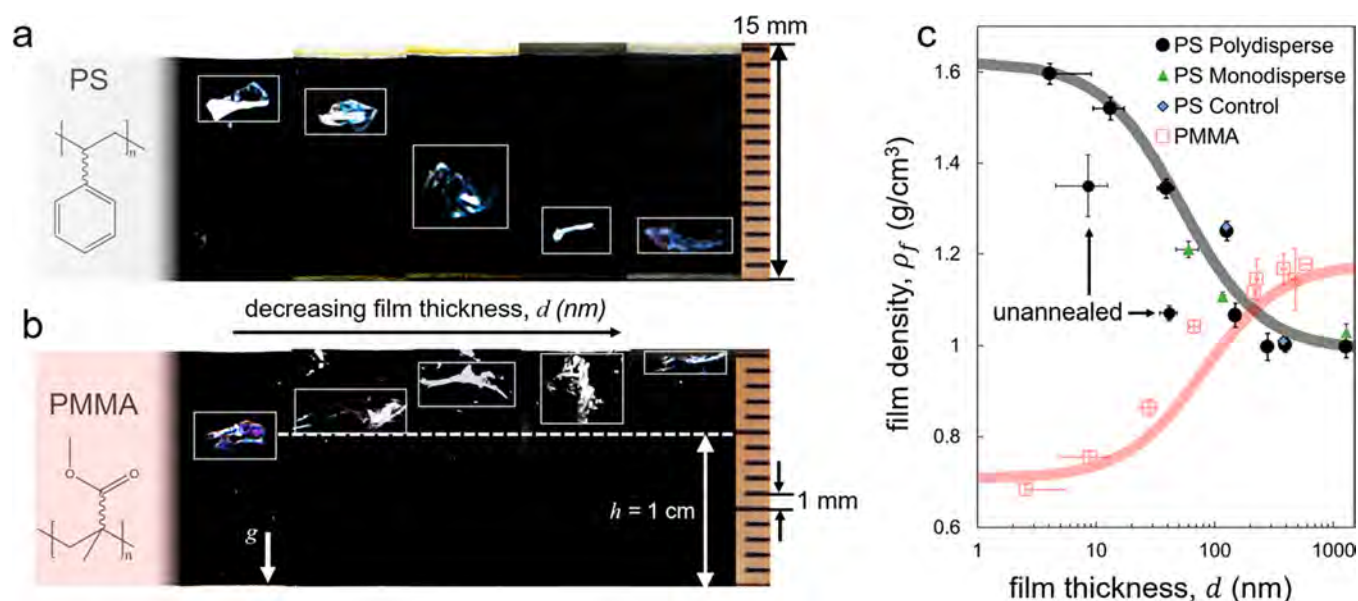


**Figure 3.** Dependence of the density of PS and PMMA films upon thickness. (a) Molecular structure and photographs of thin films of (a) PS and (b) PMMA of different thickness, magnetically levitating in the paramagnetic solution. These photographs were corrected for brightness and contrast to make the suspended film clearly visible. (c) Plot showing the mass density (obtained from magnetic levitation experiments) as a function of the thickness of the PS (both a polydisperse and monodisperse sample) and PMMA film (determined from stylus profilometry). Error bars for thickness and density represent 95% confidence intervals of the mean value from stylus profilometry ( $N = 7$ ) and MagLev measurements ( $N = 7$ ), respectively. The curves in (c) represent the best fit of eq 2 to the experimental data, obtained by a nonlinear regression of the measured density of the film to the measured thickness. “PS Control” shows data from a control experiment for the processing parameters, in which the concentration was held fixed at 17.5 mg/mL and the spin-coating speed (500, 5500 rpm) was changed to control the thickness.

films. Figure 3c shows a plot of density versus thickness obtained from the MagLev experiments. In agreement with some of the existing measurements in the literature,<sup>2–4,7,49</sup> we observed qualitatively opposite trends for PS and PMMA: the density of PS increased relative to the bulk value by a factor of 1.6, while the density of PMMA decreased by a factor 0.6, for films approximately  $\sim 4$  nm thick. (See Figure S8 for a graphical comparison to previous results; we observed qualitative matching with values inferred from measurements of the refractive index<sup>2–4,49</sup> and quantitative matching with values obtained from quartz crystal microbalance dissolution experiments.<sup>7</sup>) We view the quantitative matching between densities measured by MagLev and quartz crystal microbalance dissolution experiments as a strong validation of both approaches. For PS, we observed a larger increase in density with thickness than that previously observed with ellipsometry, with our films reaching a maximum density of 1.6 g/cm<sup>3</sup> at a thickness of 4 nm. This surprising finding is supported by previous molecular dynamics simulations by Hudzinsky *et al.*, who found that the density could reach a value of almost 2 g/cm<sup>3</sup> directly at the interface with the substrate (see Figure S9 for density profiles reproduced from these simulations).<sup>53</sup> These simulations revealed a liquid crystalline ordering of the polymer in this densified region, which we believe to be the mechanism for the effect observed in our experiments.<sup>53</sup> Similar phenomena were also observed in simulations of PS on graphitic surfaces by Lee *et al.*,<sup>54</sup> where contributions from the backbone and phenyl rings were also dissected. We note that there are oscillations in the density profile (Figure S9), so the predicted average density of the film is 1.2 g/cm<sup>3</sup> for a film with a thickness of 10 nm.<sup>53</sup> MagLev measures the mass density of the *solvent accessible* volume of the film, however, which may explain why we observe higher values of density (in

addition to limitations of molecular dynamics simulations and possible systematic error associated with MagLev).

In both cases, we observed a sigmoidal transition in density as the film approached a critical thickness, suggesting a physically important length scale, probably related to the size of the polymer chains as well as the strength of interaction with the substrate. To estimate quantitatively the length scale for the transition in density, we fit the following empirically determined function, eq 2, to the experimental data.

$$\rho_f = \rho_s + \frac{\rho_\infty - \rho_s}{\frac{d_c}{d} + 1} \quad (2)$$

Here,  $\rho_f$  (g/cm<sup>3</sup>) is the film density,  $\rho_s$  (g/cm<sup>3</sup>) is the “skin density”, and  $\rho_\infty$  (g/cm<sup>3</sup>) is the bulk density, and  $d_c$  (nm) is the critical thickness at which the transition in density occurs. The “skin density” is an empirical parameter, defined mathematically as the asymptotic density in the limit of thickness approaching zero.

A best fit of eq 2 to the experimental data, obtained by optimizing the values of  $\rho_s$  and  $d_c$ , yielded a value 52 nm for  $d_c^{\text{PS}}$  and 80 nm for  $d_c^{\text{PMMA}}$ . Given that the radii of gyration,  $R_g$ , of these two polymers, assuming an ideal chain model,<sup>55</sup> are similar ( $R_g \approx 11$  nm for PS and  $R_g \approx 9$  nm for PMMA), we expect this difference to be related to the molecular structure and the nature of the polymer–substrate interaction rather than the size of the polymer chains. More detailed experiments with monodisperse polymers of varied chain lengths would be required to show the dependency of the length scale for the transition in the density upon the radius of gyration. The best fit values for  $\rho_s$  were 1.6 g/cm<sup>3</sup> for PS and 0.7 g/cm<sup>3</sup> for PMMA.

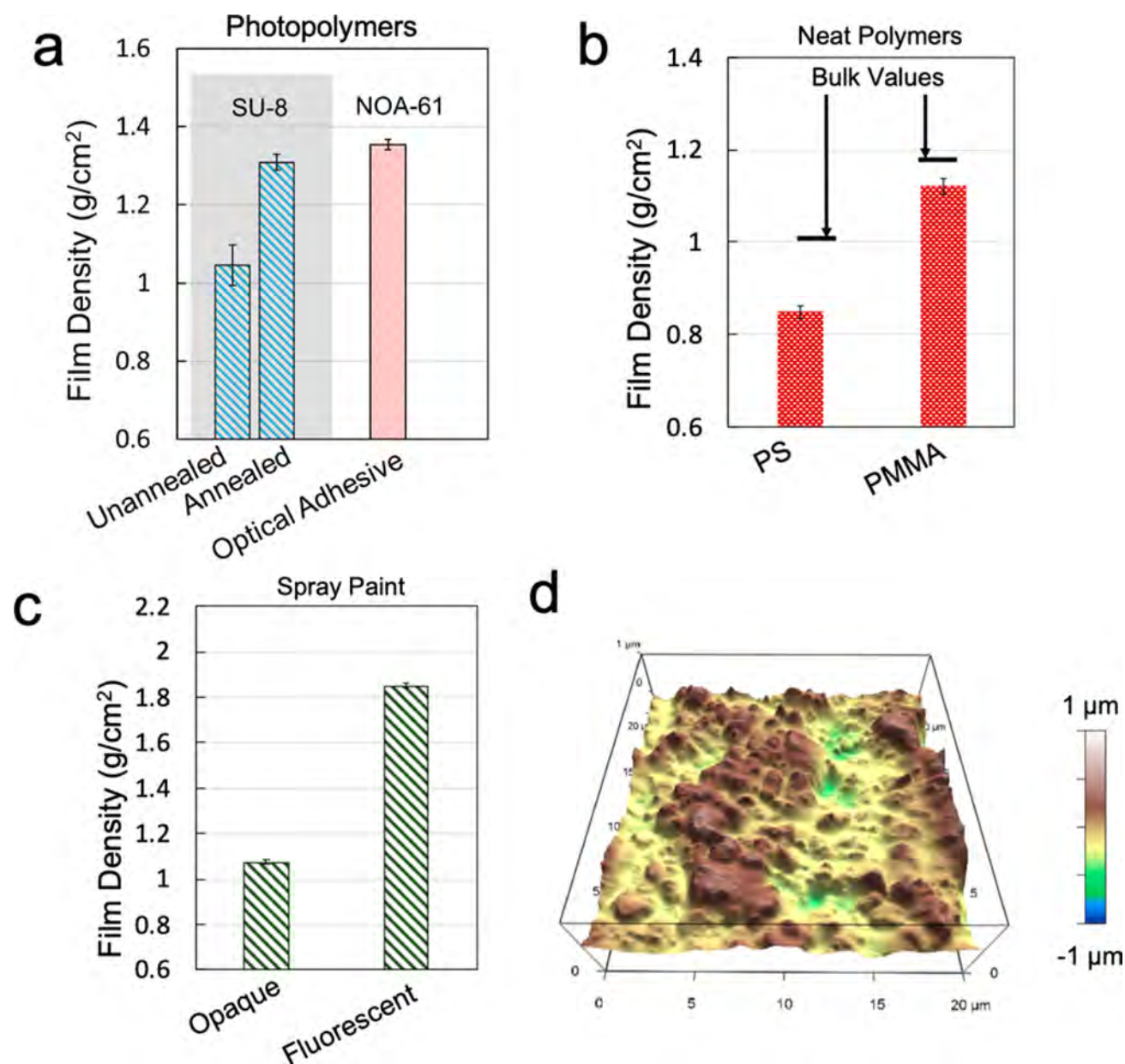


**Figure 4.** Demonstrations of the utility of MagLev for different types of polymer films. Bar charts showing measured densities for (a) two photopolymers (SU-8 photoresist, and Norland Optical Adhesive, NOA-61), (b) spray-coated films of neat polymers, (c) and spray paint. (d) Atomic force micrograph of the rough surface of a spray-cast film of fluorescent paint.

There are several potential physical mechanisms by which changes in the density of a polymer film could occur: (i) they could arise due to differences in the polymer structure in the solutions from which they are cast (*i.e.*, overlapping and entangled in concentrated solutions or isolated and unentangled in dilute solutions),<sup>2</sup> (ii) they could arise from differences in the processing of the films after casting (*i.e.*, annealing time and temperature), or (iii) they could arise due to interfacial effects.

In all cases, the films were annealed above the glass transition temperature for 12 h, so we expected the third mechanism to prevail. To test this hypothesis, we performed a control experiment with PS. Instead of varying the concentration of polymer with a constant angular velocity of the spin-coater to modify the thickness, we used a fixed concentration of dissolved polymer (17.5 mg/mL) and

changed the angular velocity to control the thickness of the film. The data from these experiments are shown with blue diamonds in Figure 3c. We found that these films followed the same trends as the films of similar thickness spun from solutions with different concentrations. Based on these observations, we concluded that the thermal annealing served to erase the processing history, and that the density variations arose from interfacial effects.<sup>2,3,11</sup>

To further explore these phenomena, we also measured the density of thin films of PS which were not thermally annealed above the glass transition temperature (*i.e.*, “as-cast films”). As shown in the data points labeled as “unannealed” in Figure 3c, we observed that without thermal annealing, the films still exhibited an increase in density relative to the bulk value, but of smaller magnitude. These results indicated that the thermal

annealing step was required to allow the polymer chains to assemble into the dense state.

As an additional control experiment, we also measured the density of a monodisperse sample of PS (with a molecular weight of 110 kDa) at several different thicknesses, shown by the green triangular data points in Figure 3c. We observed similar trends to the polydisperse sample, indicating that the observed dependence of density upon thickness was not influenced by the distribution of molecular weight of the polymer chains.

**Demonstrations of Utility.** To demonstrate that MagLev is applicable to a broad range of polymer films, we applied it to measure the density of several different classes of films. Photopolymers are one particularly important class of polymers that are typically used as photoresists in micro/nanofabrication, such as the popular epoxy-based photoresist, SU-8. The standard protocol for preparing SU-8 structures is to spin-coat a film, anneal the film to remove residual solvent (*i.e.*, “soft bake”), cure the film with exposure to UV light through a photomask, and finally apply a second annealing step (*i.e.*, a “postexposure bake”) to complete the cross-linking process. We applied MagLev to measure the density of an  $\sim 1\ \mu\text{m}$  film of SU-8 2000 before and after the final annealing step and observed a 30% increase in density following annealing. We also measured the density of a thin film of a transparent optical adhesive, NOA-61, and found a close match with the reported bulk value.<sup>56</sup>

One characteristic of a film that confounds measurements of density based on reflectometry is the roughness of the surface. Although spin-coated films are generally smooth, not all casting processes produce smooth surfaces. Another common method of casting a polymer film is by spray-coating: a process by which the polymer solution is transferred to the surface as an aerosol (*e.g.*, spray paint). We prepared neat polymer films of PS and PMMA by spray-coating from toluene. We found that both of these polymers exhibited a density lower than the bulk value when processed into a film by spray-coating. The fact that spray-cast films of PS could exhibit an increase in the levitation height (corresponding to a decrease in density) provides additional evidence to reinforce our conclusion that a chemically specific interaction between the polymer film and the ionic solution is not the cause of the observed changes in the levitation height.

Figure 4c compares the densities of spray-cast films of a typical acrylic-based paint (Krylon fusion) as well as a fluorescent formulation (ACE Glo Spray). The fluorescent formulation has a greater mass density, which may be due to the presence of an additive required to make the paint fluoresce. Figure 4d shows an atomic force micrograph of the rough surface of the fluorescent spray paint.

## CONCLUSIONS

This paper demonstrates that MagLev is a suitable method to measure the mass density of thin films (10–1000 nm) of hydrophobic polymers. MagLev is inexpensive (the apparatus costs <\$300 to construct), compact, and portable, and it does not require electricity to operate.<sup>9,45</sup> MagLev is compatible with polymer films as thin as  $\sim 3\ \text{nm}$  (as measured by stylus profilometry) and with films that have rough surfaces and/or absorb visible light strongly, characteristics that pose problems for X-ray reflectivity and ellipsometry. MagLev measures the density of the polymer films irrespective of their masses, volumes, or shapes. It directly measures density without

requiring any material-specific modeling.<sup>9,45</sup> Moreover, we establish that PAA is a suitable sacrificial release layer for carrying out this procedure.

We validated the technique by measuring the density of films of polymers ( $>100\ \text{nm}$  thick) with a broad range of densities ( $1.0\text{--}1.4\ \text{g/cm}^3$ ) and observed values that matched with the bulk density (Figure 2). We showed that confinement of these polymers to films less than  $\sim 100\ \text{nm}$  thick produced large changes in the density measure by MagLev. Detailed measurements of these density changes as a function of thickness in PS and PMMA revealed a sigmoidal dependency that matched some of the previously reported trends for PS and PMMA.<sup>2–4,7,49</sup> In particular, our measurements matched most closely with measurements of density obtained by quartz crystal microbalance dissolution experiments.<sup>7</sup> Importantly, our technique is complementary to existing methods based on measurement of the refractive index.<sup>2,3</sup> MagLev adds an alternative means for measuring the density of polymer films and allows for more information about the material to be inferred. For example, one can use the Lorentz–Lorenz equation to infer the molecular polarizability using independent measurements of the refractive index and the mass density.<sup>24</sup>

The experimental simplicity of MagLev makes it a good candidate for routine metrology in polymer science and engineering. Moreover, this technique can be directly applied to measure the density of polar polymer films, using a hydrophobic sacrificial layer and paramagnetic solution, as well as nonpolymeric films (*e.g.*, metal, oxide, or perovskite films). This approach will be useful for polymer chemists and materials scientists aiming to characterize and optimize properties of thin films formed using a variety of processes<sup>57</sup> and would help address questions in polymer science, such as the effect of interfacial confinement on the nanoscale packing of polymer chains and the macroscopic properties of thin films.

## EXPERIMENTAL METHODS

**Materials.** Ultraflat (roughness  $< 0.5\ \text{nm}$ ) *p*-type silicon wafers (2 in. diameter) were purchased from Alpha Nanotech Inc. (ANUF0S00S2). Polydisperse polystyrene (PS,  $M_n = 170\ 000\ \text{Da}$ , PDI = 2.04, 441147-1KG, Batch # 04612CJ) was purchased from Sigma-Aldrich. Poly(methyl methacrylate) (PMMA,  $M_n = 75\ 000\ \text{Da}$ , PDI = 2.8, CAT # 04553, LOT # 552464) was purchased from Polysciences Inc. Monodisperse PS ( $M_n = 110\ 000\ \text{Da}$ , PDI = 1.03, Lot # ps100313wa) was purchased from Polymer Standards Service-USA, Inc. Polyvinyl chloride (PVC,  $M_n = \text{high}$ , PDI = *unknown*, 81392-10G), poly(ether imide) (PEI,  $M_n = \text{unknown}$ , PDI = *unknown*, 700193-250G, LOT # MKBC0294 V), and poly(isobutyl methacrylate) (PIBMA,  $M_w = 70\ 000\ \text{Da}$ , 181544-250G, Batch # 04926MH) were purchased from Sigma-Aldrich Inc. Polyacrylic acid (PAA,  $M_n \sim 5000$ ) was purchased from Polysciences Inc. in a 50% by mass aqueous solution and then diluted to 15% by mass aqueous solution by adding deionized water. SU-8 2000.5 photoresist was purchased from Kayaku Advanced Materials, Inc. (formerly MicroChem Corp.). NOA-61 optical adhesive was purchased from Norland Products.

**Preparation of Films.** For PS, PMMA, and PIBMA, a stock solution was prepared in toluene at a concentration of 100 mg/mL (that is, 10 mg of solid polymer per mL of solvent) by stirring overnight at a temperature of 50 °C and then passing the solution through a PTFE syringe filter (pore size: 1  $\mu\text{m}$ ). Solutions with 75, 50, 25, 17.5, 10, 5, and 1 mg/mL concentrations were prepared via serial dilution using a 5 mL Hamilton glass syringe.

For PEI or PVC, a stock solution was prepared in *N*-methyl-2-pyrrolidone at a concentration of 100 mg/mL by stirring overnight at a temperature of 50 °C and then passing the solution through a PTFE



syringe filter (pore size: 1  $\mu\text{m}$ ). Then solutions with 50 and 10 mg/mL concentrations for PVC and 100 and 10 mg/mL concentrations for PEI were prepared via serial dilution using a 5 mL Hamilton glass syringe.

Prior to spin-coating, silicon wafers were sequentially sonicated in deionized water containing Alconox detergent ( $\sim 1$  mg/mL), neat, deionized water (Milli-Q,  $<18\text{M}\Omega$ ), acetone, and isopropyl alcohol (for 5 min each) and then dried under nitrogen gas and cleaned with an air plasma in a Harrick plasma chamber at high power (18 W) for 5 min. Spin-coating (PWM32, Headway Research Inc., Garland, Texas) was performed both in a clean room to avoid contamination with dust particles and in a normal laboratory environment. Similar results were obtained from both sets of experiments. Films were cast by first coating the substrate with a liquid layer (2–3 mL) and then spinning them at a speed of 3000 rpm for 2 min, with a ramp of 100 rpm/s. This procedure was used for both the PAA sacrificial layer and the hydrophobic polymer layer above it. After spin-coating, films were annealed in a vacuum (approximate pressure of  $10^{-4}$  Torr) oven at 160  $^{\circ}\text{C}$  for 12 h. The only exception to this thermal annealing protocol was PVC, which was annealed at 60  $^{\circ}\text{C}$  to prevent thermal degradation, as indicated by discoloration in films annealed at higher temperature.

**Measurements of Thickness.** Thickness of films was determined by stylus profilometry with a 12  $\mu\text{m}$  diamond tip (DektakXT, Bruker, Billerica, Massachusetts) at a normal force of 1 mg. A step edge was created in the center of the silicon wafer by gently scraping it with a razor blade. The reported thicknesses of the films are the average of seven independent measurements. The measurements were performed on one polymeric film (while it was attached to wafer) for each type of polymer.

**Density-Based Measurements using MagLev.** MagLev were performed in aqueous solutions of manganese(II) chloride tetrahydrate of different concentrations for PS (2.3 M), PMMA (3.5 M), PVC (3.5 M), PEI (3.5 M), and PIBMA (3.5 M).

**Specifications of Axial MagLev Device.** The “axial MagLev” device uses two like-poles facing ring magnets (NdFeB permanent magnets, N45 grade, OD  $\times$  ID  $\times$  H: 76.2 mm  $\times$  25.4 mm  $\times$  25.4 mm) positioned coaxially with a separation of 15.0 mm. The magnets were bought from [kjmagnetics.com](http://kjmagnetics.com). The magnets are fixed in 3D printed (Stratasys Fortus 250mc, Eden Prairie, MN) holders made of acrylonitrile-butadiene-styrene-plastic (ABS) that were designed with the software Solidworks. Four threaded stainless-steel rods with hex nuts are used to hold the holders in position. The ends of the stainless-steel rods are topped with cap nuts. A standard plastic cuvette (45 mm in height) is used to levitate the diamagnetic samples in a paramagnetic medium (aqueous solutions of  $\text{MnCl}_2$  in all experiments reported here). The strength of the magnetic field (0.33 T) was measured with a DC gauss-meter (model GM1-ST; AlphaLab, Inc., Salt Lake City, UT) at the center of the top face of the bottom magnet. See Figure S10 for a photograph of the MagLev device.

**Procedure for Measurements with MagLev.** After cutting the 2” diameter wafer into  $\sim 0.25$   $\text{cm}^2$  squares using a diamond scribe, the sample was placed in a cuvette filled with an aqueous solution of  $\text{MnCl}_2$ . The cuvette was then placed in the MagLev device. After the sacrificial layer dissolved, the film floated up and equilibrated at a stable levitation height. The time for the delamination process depended upon the material, thickness, and annealing protocol and ranged from 1 min to several hours. We found no difference in the measured density of the film if it was delaminated inside or outside the MagLev device. We could not reliably measure films  $< 3$  nm thick because they were extremely delicate (*i.e.*, they broke into small pieces during the delamination process) and were difficult to observe levitating in the paramagnetic medium. We found that films delaminated more rapidly (seconds to hours, depending on thickness and annealing conditions) in deionized water than aqueous solutions of  $\text{MnCl}_2$  (minutes to hours, depending on thickness and annealing conditions). Films that delaminated in deionized water, and that then were transferred to the cuvette containing aqueous  $\text{MnCl}_2$  solution, resulted in the same density as films that delaminated in aqueous solutions of  $\text{MnCl}_2$ .

**FTIR-ATR Analysis of Polystyrene Films and Controls.** The spin-coated polystyrene films ( $\sim 1$   $\mu\text{m}$  thick) and the controls (*i.e.*, polystyrene pellets and films of PAA) were analyzed in their dry state at ambient conditions with Fourier transform infrared spectroscopy (FTIR-ATR Bruker Platinum, Bruker, Billerica, MA) with an attenuated total reflection (ATR) diamond window. We measured spectra between 4000 and 400  $\text{cm}^{-1}$  at a resolution of 4  $\text{cm}^{-1}$  with 64 sample and background scans (Figure S7).

## ASSOCIATED CONTENT

### Supporting Information

The Supporting Information is available free of charge at <https://pubs.acs.org/doi/10.1021/acsnano.1c04798>.

Tabulated Data, calibration curves, supplemental data, detailed comparison to prior results (PDF)

## AUTHOR INFORMATION

### Corresponding Author

George M. Whitesides – Department of Chemistry and Chemical Biology, Harvard University, Cambridge, Massachusetts 02138, United States; [orcid.org/0000-0001-9451-2442](https://orcid.org/0000-0001-9451-2442); Email: [gwhitesides@gmwgroup.harvard.edu](mailto:gwhitesides@gmwgroup.harvard.edu)

### Authors

Samuel E. Root – Department of Chemistry and Chemical Biology, Harvard University, Cambridge, Massachusetts 02138, United States

Rui Gao – Department of Chemistry and Chemical Biology, Harvard University, Cambridge, Massachusetts 02138, United States

Christoffer K. Abrahamsson – Department of Chemistry and Chemical Biology, Harvard University, Cambridge, Massachusetts 02138, United States

Mohamad S. Kodaimati – Department of Chemistry and Chemical Biology, Harvard University, Cambridge, Massachusetts 02138, United States

Shencheng Ge – Department of Chemistry and Chemical Biology, Harvard University, Cambridge, Massachusetts 02138, United States

Complete contact information is available at: <https://pubs.acs.org/doi/10.1021/acsnano.1c04798>

### Author Contributions

<sup>†</sup>S.E.R. and R.G. contributed equally to this work.

### Notes

The authors declare no competing financial interest.

## ACKNOWLEDGMENTS

The early stage of this work was funded by the U.S. Department of Energy, Office of Basic Energy Sciences, Division of Materials Sciences and Engineering under Award Number ER45852. Sample preparation and characterization was performed in part at the Center for Nanoscale Systems (CNS) at Harvard University, a member of the National Nanotechnology Infrastructure Network (NNIN), which is supported by the National Science Foundation (ECS0335765). We would like to thank Prof. Connie Roth and Yixuan Han for the useful discussions that led us to perform additional control experiments.

## REFERENCES

- (1) Fleer, G. J.; Cohen Stuart, M. A.; Scheutjens, J. M. H. M.; Cosgrove, T.; Vincent, B. *Polymers at Interfaces*; Chapman & Hall: London, 1998.
- (2) Ata, S.; Kuboyama, K.; Ito, K.; Kobayashi, Y.; Ougizawa, T. Anisotropy and Densification of Polymer Ultrathin Films as Seen by Multi-Angle Ellipsometry and X-Ray Reflectometry. *Polymer* **2012**, *53*, 1028–1033.
- (3) Vignaud, G.; Chebil, M. S.; Bal, J. K.; Delorme, N.; Beuvier, T.; Grohens, Y.; Gibaud, A. Densification and Depression in Glass Transition Temperature in Polystyrene Thin Films. *Langmuir* **2014**, *30*, 11599–11608.
- (4) Unni, A. B.; Vignaud, G.; Chapel, J. P.; Giermanska, J.; Bal, J. K.; Delorme, N.; Beuvier, T.; Thomas, S.; Grohens, Y.; Gibaud, A. Probing the Density Variation of Confined Polymer Thin Films via Simple Model-Independent Nanoparticle Adsorption. *Macromolecules* **2017**, *50*, 1027–1036.
- (5) Huang, X.; Roth, C. B. Changes in the Temperature-Dependent Specific Volume of Supported Polystyrene Films with Film Thickness. *J. Chem. Phys.* **2016**, *144*, 234903.
- (6) Han, Y.; Huang, X.; Rohrbach, A. C. W.; Roth, C. B. Comparing Refractive Index and Density Changes with Decreasing Film Thickness in Thin Supported Films across Different Polymers. *J. Chem. Phys.* **2020**, *153*, 044902.
- (7) Giermanska, J.; Ben Jabrallah, S.; Delorme, N.; Vignaud, G.; Chapel, J. P. Direct Experimental Evidences of the Density Variation of Ultrathin Polymer Films with Thickness. *Polymer* **2021**, *228*, 123934.
- (8) Russell, T. P.; Chai, Y. 50th Anniversary Perspective: Putting the Squeeze on Polymers: A Perspective on Polymer Thin Films and Interfaces. *Macromolecules* **2017**, *50*, 4597–4609.
- (9) Ge, S.; Nemiroski, A.; Mirica, K. A.; Mace, C. R.; Hennek, J. W.; Kumar, A. A.; Whitesides, G. M. Magnetic Levitation in Chemistry, Materials Science, and Biochemistry. *Angew. Chem., Int. Ed.* **2020**, *59* (41), 17810–17855.
- (10) Xie, J.; Zhao, P.; Zhang, C.; Fu, J.; Turng, L. S. Current State of Magnetic Levitation and Its Applications in Polymers: A Review. *Sens. Actuators, B* **2021**, *333*, 129533.
- (11) Keddie, J. L.; Jones, R. A. L.; Cory, R. A. Size-Dependent Depression of the Glass Transition Temperature in Polymer Films. *Epl* **1994**, *27*, 59–64.
- (12) Priestley, R. D.; Ellison, C. J.; Broadbelt, L. J.; Torkelson, J. M. Structural Relaxation of Polymer Glasses at Surfaces, Interfaces, and in Between. *Science* **2005**, *309*, 456–459.
- (13) Fakhraei, Z.; Forrest, J. A. Measuring the Surface Dynamics of Glassy Polymers. *Science* **2008**, *319*, 600–604.
- (14) Gu, X.; Shaw, L.; Gu, K.; Toney, M. F.; Bao, Z. The Meniscus-Guided Deposition of Semiconducting Polymers. *Nat. Commun.* **2018**, *9*, 534.
- (15) Abrahamsson, C.; Ge, S.; Bell, J.; Blackledge, R.; Whitesides, G. M. Density Determination and Separation via Magnetic Levitation. In *FORENSIC ANALYSIS ON THE CUTTING EDGE: More New Methods for Trace Evidence Analysis*; John Wiley & Sons: Hoboken, NJ, 2021; Chapter 4.
- (16) Priestley, R. D.; Cangialosi, D.; Napolitano, S. On the Equivalence between the Thermodynamic and Dynamic Measurements of the Glass Transition in Confined Polymers. *J. Non-Cryst. Solids* **2015**, *407*, 288–295.
- (17) Jones, R. L.; Kumar, S. K.; Ho, D. L.; Briber, R. M.; Russell, T. P. Chain Conformation in Ultrathin Polymer Films. *Nature* **1999**, *400*, 146–149.
- (18) Jones, R. L.; Kumar, S. K.; Ho, D. L.; Briber, R. M.; Russell, T. P. Chain Conformation in Ultrathin Polymer Films Using Small-Angle Neutron Scattering. *Macromolecules* **2001**, *34*, 559–567.
- (19) De Gennes, P. G. Glass Transitions in Thin Polymer Films. *Eur. Phys. J. E: Soft Matter Biol. Phys.* **2000**, *2*, 201–205.
- (20) Frank, C. W.; Rao, V.; Despotopoulou, M. M.; Pease, R. F. W.; Hinsberg, W. D.; Miller, R. D.; Rabolt, J. F. Structure in Thin and Ultrathin Spin-Cast Polymer Films. *Science* **1996**, *273*, 912–915.
- (21) Forrest, J. A.; Dalnoki-Veress, K.; Stevens, J. R.; Dutcher, J. R. Effect of Free Surfaces on the Glass Transition Temperature of Thin Polymer Films. *Phys. Rev. Lett.* **1996**, *77*, 2002–2005.
- (22) Dalnoki-Veress, K.; Forrest, J. A.; Murray, C.; Gigault, C.; Dutcher, J. R. Molecular Weight Dependence of Reductions in the Glass Transition Temperature of Thin, Freely Standing Polymer Films. *Phys. Rev. E: Stat. Phys., Plasmas, Fluids, Relat. Interdiscip. Top.* **2001**, *63*, 031801.
- (23) Kawana, S.; Jones, R. A. L. Character of the Glass Transition in Thin Supported Polymer Films. *Phys. Rev. E: Stat. Phys., Plasmas, Fluids, Relat. Interdiscip. Top.* **2001**, *63* (6), 021501–1–6.
- (24) Ellison, C. J.; Ruzsokowski, R. L.; Fredin, N. J.; Torkelson, J. M. Dramatic Reduction of the Effect of Nanoconfinement on the Glass Transition of Polymer Films via Addition of Small-Molecule Diluent. *Phys. Rev. Lett.* **2004**, *92*, 095702.
- (25) Ellison, C. J.; Mundra, M. K.; Torkelson, J. M. Impacts of Polystyrene Molecular Weight and Modification to the Repeat Unit Structure on the Glass Transition-Nanoconfinement Effect and the Cooperativity Length Scale. *Macromolecules* **2005**, *38*, 1767–1778.
- (26) Evans, C. M.; Deng, H.; Jager, W. F.; Torkelson, J. M. Fragility Is a Key Parameter in Determining the Magnitude of  $T_g$ -Confinement Effects in Polymer Films. *Macromolecules* **2013**, *46*, 6091–6103.
- (27) Hsu, D. D.; Xia, W.; Song, J.; Keten, S. Glass-Transition and Side-Chain Dynamics in Thin Films: Explaining Dissimilar Free Surface Effects for Polystyrene vs Poly(Methyl Methacrylate). *ACS Macro Lett.* **2016**, *5*, 481–486.
- (28) Forrest, J. A.; Dalnoki-Veress, K. The Glass Transition in Thin Polymer Films. *Adv. Colloid Interface Sci.* **2001**, *94*, 167–195.
- (29) Zanten, J. H.; Van Wallace, W. E.; Wu, W. Effect of Strongly Favorable Substrate Interactions on the Thermal Properties of Ultrathin Polymer Films. *Phys. Rev. E* **1996**, *53*, 2053–2056.
- (30) Kremer, F.; Tress, M.; Mapesa, E. U. Glassy Dynamics and Glass Transition in Nanometric Layers and Films: A Silver Lining on the Horizon. *J. Non-Cryst. Solids* **2015**, *407*, 277–283.
- (31) Zhang, W.; Douglas, J. F.; Starr, F. W. Why We Need to Look beyond the Glass Transition Temperature to Characterize the Dynamics of Thin Supported Polymer Films. *Proc. Natl. Acad. Sci. U. S. A.* **2018**, *115*, 5641–5646.
- (32) Reiter, G. Mobility of Polymers in Films Thinner than Their Unperturbed Size. *Epl* **1993**, *23*, 579–584.
- (33) Wallace, W. E.; Beck Tan, N. C.; Wu, W. L.; Satija, S. Mass Density of Polystyrene Thin Films Measured by Twin Neutron Reflectivity. *J. Chem. Phys.* **1998**, *108*, 3798–3804.
- (34) Stafford, C. M.; Harrison, C.; Beers, K. L.; Karim, A.; Amis, E. J.; Vanlandingham, M. R.; Kim, H. C.; Volksen, W.; Miller, R. D.; Simonyi, E. E. A Buckling-Based Metrology for Measuring the Elastic Moduli of Polymeric Thin Films. *Nat. Mater.* **2004**, *3*, 545–550.
- (35) Chung, J. Y.; Lee, J. H.; Beers, K. L.; Stafford, C. M. Stiffness, Strength, and Ductility of Nanoscale Thin Films and Membranes: A Combined Wrinkling-Cracking Methodology. *Nano Lett.* **2011**, *11*, 3361–3365.
- (36) Alkhadra, M. A.; Root, S. E.; Hilby, K. M.; Rodriguez, D.; Sugiyama, F.; Lipomi, D. J. Quantifying the Fracture Behavior of Brittle and Ductile Thin Films of Semiconducting Polymers. *Chem. Mater.* **2017**, *29*, 10139–10149.
- (37) Root, S. E.; Alkhadra, M. A.; Rodriguez, D.; Printz, A. D.; Lipomi, D. J. Measuring the Glass Transition Temperature of Conjugated Polymer Films with Ultraviolet-Visible Spectroscopy. *Chem. Mater.* **2017**, *29* (7), 2646–2654.
- (38) Huang, J.; Juskiewicz, M.; de Jeu, W. H.; Cerda, E.; Emrick, T.; Menon, N.; Russell, T. P. Capillary Wrinkling of Floating Thin Polymer Films. *Science* **2007**, *317*, 650–653.
- (39) Kim, J.-H.; Nizami, A.; Hwangbo, Y.; Jang, B.; Lee, H.-J.; Woo, C.-S.; Hyun, S.; Kim, T.-S. Tensile Testing of Ultra-Thin Films on Water Surface. *Nat. Commun.* **2013**, *4*, 2520.
- (40) Liu, Y.; Chen, Y. C.; Hutchens, S.; Lawrence, J.; Emrick, T.; Crosby, A. J. Directly Measuring the Complete Stress-Strain Response of Ultrathin Polymer Films. *Macromolecules* **2015**, *48*, 6534–6540.

- (41) Rodriquez, D.; Kim, J.-H.; Root, S. E.; Fei, Z.; Boufflet, P.; Heeney, M.; Kim, T.-S.; Lipomi, D. J. Comparison of Methods for Determining the Mechanical Properties of Semiconducting Polymer Films for Stretchable Electronics. *ACS Appl. Mater. Interfaces* **2017**, *9* (10), 8855–8862.
- (42) Lipomi, D. J.; Tee, B. C.-K.; Vosgueritchian, M.; Bao, Z. Stretchable Organic Solar Cells. *Adv. Mater.* **2011**, *23*, 1771–1775.
- (43) Root, S. E.; Savagatrup, S.; Printz, A. D.; Rodriquez, D.; Lipomi, D. J. Mechanical Properties of Organic Semiconductors for Stretchable, Highly Flexible, and Mechanically Robust Electronics. *Chem. Rev.* **2017**, *117*, 6467–6499.
- (44) Lee, J. H.; Chung, J. Y.; Stafford, C. M. Effect of Confinement on Stiffness and Fracture of Thin Amorphous Polymer Films. *ACS Macro Lett.* **2012**, *1*, 122–126.
- (45) Mirica, K. A.; Shevkopyas, S. S.; Phillips, S. T.; Gupta, M.; Whitesides, G. M. Measuring Densities of Solids and Liquids Using Magnetic Levitation: Fundamentals. *J. Am. Chem. Soc.* **2009**, *131*, 10049–10058.
- (46) Khodaparast, S.; Boulogne, F.; Poulard, C.; Stone, H. A. Water-Based Peeling of Thin Hydrophobic Films. *Phys. Rev. Lett.* **2017**, *119*, 154502.
- (47) Linder, V.; Gates, B. D.; Ryan, D.; Parviz, B. A.; Whitesides, G. M. Water-Soluble Sacrificial Layers for Surface Micromachining. *Small* **2005**, *1*, 730–736.
- (48) Ge, S.; Whitesides, G. M. Axial<sup>™</sup> Magnetic Levitation Using Ring Magnets Enables Simple Density-Based Analysis, Separation, and Manipulation. *Anal. Chem.* **2018**, *90*, 12239–12245.
- (49) Wu, W.-L.; Orts, W. J.; Van Zanten, J. H.; Fanconi, B. M. Density Profile of Spin Cast Polymethylmethacrylate Thin Films. *J. Polym. Sci., Part B: Polym. Phys.* **1994**, *32*, 2475–2480.
- (50) Van der Lee, A.; Hamon, L.; Holl, Y.; Grohens, Y. Density Profiles in Thin PMMA Supported Films Investigated by X-Ray Reflectometry. *Langmuir* **2001**, *17*, 7664–7669.
- (51) Simpson, G. J.; Sedin, D. L.; Rowlen, K. L. Surface Roughness by Contact *versus* Tapping Mode Atomic Force Microscopy. *Langmuir* **1999**, *15*, 1429–1434.
- (52) Alkindi, A. S.; Al-Wahaibi, Y. M.; Muggeridge, A. H. Physical Properties (Density, Excess Molar Volume, Viscosity, Surface Tension, and Refractive Index) of Ethanol + Glycerol. *J. Chem. Eng. Data* **2008**, *53*, 2793–2796.
- (53) Hudzinsky, D.; Lyulin, A. V.; Baljon, A. R. C.; Balabaev, N. K.; Michels, M. A. J. Effects of Strong Confinement on the Glass-Transition Temperature in Simulated Atactic Polystyrene Films. *Macromolecules* **2011**, *44*, 2299–2310.
- (54) Lee, S.; Lyulin, A. V.; Frank, C. W.; Yoon, D. Y. Interface Characteristics of Polystyrene Melts in Free-Standing Thin Films and on Graphite Surface from Molecular Dynamics Simulations. *Polymer* **2017**, *116*, 540–548.
- (55) Hiemenz, P. C.; Lodge, T. P. *Polymer Chemistry*; CRC Press, Boca Raton, FL, 2007.
- (56) Norland Products Incorporated. *Norland Optical Adhesives 61 Datasheet*. <https://www.norlandprod.com/literature/61tds.pdf> (accessed 2021-08-09).
- (57) Runser, R.; Root, S. E.; Ober, D. E.; Choudhary, K.; Chen, A. X.; Dhong, C.; Urbina, A. D.; Lipomi, D. J. Interfacial Drawing: Roll-to-Roll Coating of Semiconducting Polymer and Barrier Films onto Plastic Foils and Textiles. *Chem. Mater.* **2019**, *31*, 9078–9086.